ChemPubSoc Europe

DOI: 10.1002/cplu.201300244

0D to 1D Switching of Hybrid Polyoxometalate Assemblies at the Nanoscale by Using Molecular Control

Wei Chen,[a] Dui Ma,[a] Jun Yan,[b] Thomas Boyd,[b] Leroy Cronin,[b] De-Liang Long,[b] and Yu-Fei Song*[a]

The control of assembly of polyoxometalates (POMs)[1–3] across length scales is challenging because it requires the manipulation of molecular architecture, supramolecular interactions and the physicochemical properties of the assemblies.[4,5] In this respect, the development of novel POM-based organic/inorganic hybrids has focused on the functionality of hybrid materials with improved applications-driven performance and/or other useful physical properties in recent years.[1,2,6] One effective pathway for the design of POM assemblies is to covalently tether functional organic components onto POMs.[2,7] For example, the incorporation of structural motifs that are responsive to external stimuli onto the POMs allows the generation of POM-containing functional hybrid materials.[8] In comparison to conventional POMs, these new POM-containing hybrids involve π–π and van der Waals interactions, which play crucial roles for a better understanding of self-assembly processes and thereby the formations of novel aggregates.[4,7,9,10]

In 2008, some of us reported,[7b] for the first time, POM-containing amphiphiles, in which a Mn–Anderson cluster was covalently functionalised with various alkyl chains. It was demonstrated that these amphiphiles showed the formation of unusual vesicle-like structures. Later, Polarz et al. reported a new class of surfactants with a mono-lacunary cluster of $[PW_{11}O_{39}]^{x}$ as the head group; these amphiphiles were catalytically active.[6a] The next level of complexity was fulfilled by the design of bimetallic ruthenium-containing amphiphiles with POM as the head group.[6b] As such, Polarz et al. reported surfactants containing two different transition metals, tungsten and ruthenium, which exhibited reversible electrochemical switching from spherical to rod-like micelles.[6b] It is worthwhile noting the example by Winnik et al.,[11] who showed that the combination of self-assembly and stimuli-responsive properties was a rather unexplored area. Interestingly, Wu et al. reported a surfactant-encapsulated photo-responsive POM complex, which exhibited fibre-like morphology in its *trans* state and a spherical structure upon UV irradiation.[12] Nevertheless, the number of studies on the response of amphiphilic aggregates to external factors is limited.

Based on a previous design strategy of amphiphiles with hydrophilic POM head groups attached to hydrophobic alkyl tails, the incorporation of photo-responsive entities with π–π interactions into the designed amphiphiles may affect their assembly behaviour. As a result, a series of POM-based assemblies with different covalently grafted alkyl chains terminated with photo-responsive azobenzene moieties have been prepared, and an investigation into their assembly behaviour in co-solvent has been performed.

Three organic/inorganic hybrid assemblies with the general molecular formula of $[C_{16}H_{36}N]_4[SiW_{11}O_{40}(SiCH_2CH_2CH_2NH{-}CO{-}(CH_2)_nO{-}C_6H_4N{=}NC_6H_5)_2]$ ($n=0$ (**1**), 5 (**2**) and 10 (**3**)) have been prepared (Scheme 1), in which azobenzene moieties and alkyl

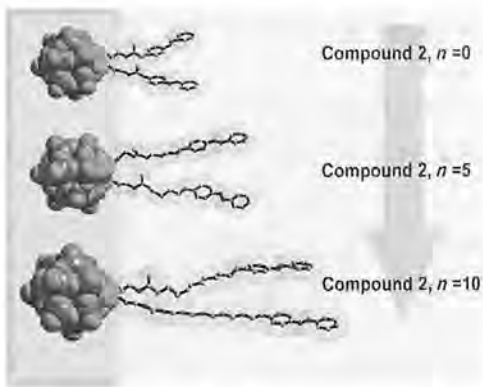

Scheme 1. Schematic representation of compounds **1**, **2** and **3** with molecular structures of $[C_{16}H_{36}N]_4[SiW_{11}O_{40}(SiCH_2CH_2CH_2NHCO(CH_2)_nO{-}C_6H_4N{=}NC_6H_5)_2]$ ($n=0$ (**1**), 5 (**2**) and 10 (**3**)).

chains have been covalently anchored onto both sides of $[C_{16}H_{36}N]_4[SiW_{11}O_{40}(SiCH_2CH_2CH_2NH_2{\cdot}HCl)_2]$ (Figure S1 in the Supporting Information).[13] ^1H and ^{13}C NMR spectroscopy, ESI-MS, FTIR spectroscopy and elemental analysis results fully support the successful preparation of compounds **2** and **3**.

The ESI-MS measurement contains two signals at *m/z* 1777.31 and 1897.97, which correspond to $[1-3TBA+H]^{2+}$ (TBA = tetrabutylammonium) and $[1-2TBA]^{2+}$ (Figure S2 in the Supporting Information) for compound **1**. In the case of compound **2** (Figure 1), two signals at *m/z* 1846.34 and 1967.96 are assigned to $[2-3TBA+H]^{2+}$ and $[2-2TBA]^{2+}$, respectively, which are in good agreement with the calculated isotopic molecular mass. The ESI-MS spectrum of compound **3** contains

[a] W. Chen, D. Ma, Prof. Y.-F. Song
State Key Laboratory of Chemical Resource Engineering,
Beijing University of Chemical Technology,
Beijing 100029 (P.R. China)
Fax: (+86) 10-64431832
E-mail: songyufei@hotmail.com

[b] J. Yan, T. Boyd, Prof. L. Cronin, Dr. D.-L. Long
WestCHEM, Department of Chemistry
The University of Glasgow
Glasgow G12 8QQ (UK)

Supporting information for this article is available on the WWW under http://dx.doi.org/10.1002/cplu.201300244.

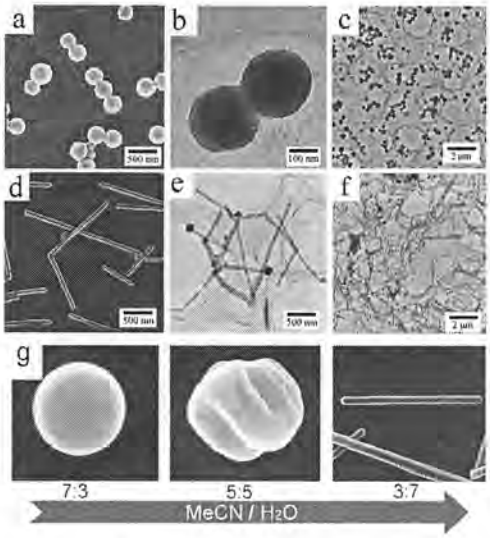

Figure 3. Compound **3** in $CH_3CN/H_2O = 7:3$: SEM (a) and TEM images (b and c). compound **3** in $CH_3CN/H_2O = 3:7$: SEM (d) and TEM images (e and f). g) the change in morphology and dimension with a decrease in the CH_3CN/H_2O ratio from 7:3 to 5:5 to 3:7.

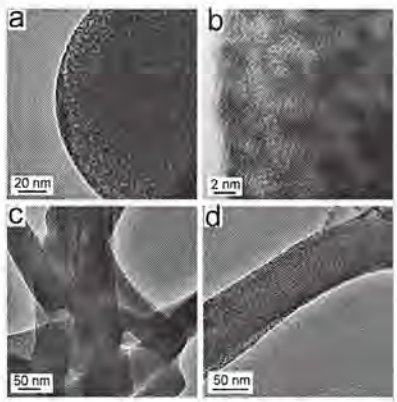

Figure 4. HRTEM images of compound **3** in $CH_3CN/H_2O = 7:3$ (a and b) and 3:7 (c and d).

that the nanorods are composed of highly ordered lamellar structures with clear light and shade boundaries. These nanorods are formed by bundles of parallel nanofibres. The distance between two neighbouring layers is 3.96 nm, which is in good agreement with the calculated diameter of compound **3**.

It is known that two opposing forces control self-association and/or aggregation of the amphiphilic molecules, in which hydrophobic interactions favour aggregation and head group interactions work in the opposite sense.[14] The geometric treatment of aggregation of the amphiphiles relates the overall free energy of association to three critical geometric characteristics of the molecule:[12,13] 1) the minimum interfacial area occupied by the surfactant hydrophilic or head group, a_0; 2) the volume of the hydrophobic tail, v; and 3) the maximum extended chain length of the tail in a "fluid" environment, such as the core of a micelle, l_c. The critical packing parameter, P_c, can be defined by Equation (1):[14]

$$P_c = v/(a_0 l_c) \quad (1)$$

The three molecular parameters allow us to predict the shape and size of aggregates that will produce a minimum in free energy. In detail, spherical micelles can be formed if $P_c < 0.33$, and cylindrical or disk-shaped micelles can be obtained if $0.33 \leq P_c \leq 0.5$.

In the case of compounds **1–3**, control experiments have been performed to evaluate the influence of water content on the morphologies and thereby the dimensions of compounds **1–3** in the CH_3CN/H_2O co-solvents. For compounds **1** and **2**, along with the increase in the water content of the solvent, the formation of spherical morphologies for both compounds in different ratios of CH_3CN/H_2O has been observed; this indicates that the molecular association of **1** and **2** does not change significantly with the change in the ratios of CH_3CN/H_2O. In contrast, with the increase of the alkyl chains from $n = 0$ (**1**) to 5 (**2**) and 10 (**3**), compound **3** shows clear morphological variation with the change in the polarity of the co-solvents. Only spherical inverted-micelles are formed at $CH_3CN/H_2O = 8:2$, 7:3 and 6:4. The increase of water content to $CH_3CN/H_2O = 5:5$ leads to curvature on the surface of the aggregate structure. Further increase of the water content until $CH_3CN/H_2O = 3:7$ and 2:8, results in the formation of nanorods. The formation of rod-like aggregates is controlled kinetically by the distribution of water during self-assembly of the hybrids in CH_3CN and H_2O co-solvent mixtures. These morphologies differ in the degree of core chain stretching and interfacial tension between the micelle core and the surrounding solvent. The above experiments suggest that the co-solvent mixture has a significant effect on the resulting morphologies in CH_3CN/H_2O co-solvents.[15,16]

As shown in Figure 5, in addition to the POM head group and hydrophobic alkyl chains, the designed POM assemblies contain azobenzene moieties with π–π interactions. Contrast experiments with those compounds without azobenzene moieties, similar to those reported by Polarz et al.,[6] show that no such controlled morphology variations with the change in co-solvent ratio can be observed. Moreover, experimental results obtained by replacing azobenzene moieties with benzene rings indicate that no such controlled assemblies with various morphologies can be obtained upon changing the co-solvent ratio. This result suggests that not simple π–π interactions can generate such experimental results, and the presence of azobenzene entities does play a role for the observed phenomena.

In summary, amphiphilic POM hybrids based on covalent functionalisation of the structural motif of $[C_{16}H_{36}N]_4[SiW_{11}O_{40}(SiCH_2CH_2CH_2NH_2{\cdot}HCl)_2]$ by different lengths of alkyl chains $n = 0$, 5 or 10 have been successfully prepared and fully characterised. The assembly behaviour could be affected by the presence of weak interactions (hydrophobic and π–π interactions) in the designed POM assemblies. Furthermore, the assembly behaviour of the amphiphilic POM hybrids could be adjusted by using different ratios of CH_3CN/H_2O, which allowed switching between 0D and 1D structures. As such, the assembly of covalently modified POMs into controllable nano-archi-

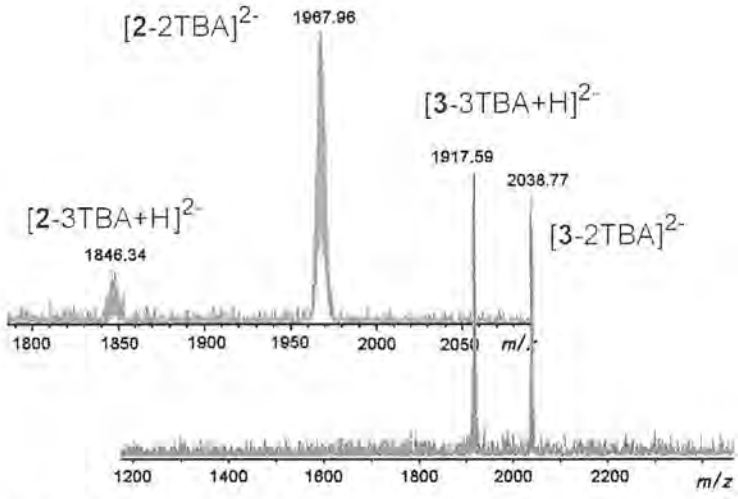

Figure 1. ESI-MS results for compounds **2** and **3**.

two signals at 1917.59 and 2038.77 which could be assigned to be $[3-3TBA+H]^{2-}$ and $[3-2TBA]^{2-}$, respectively (Figure 1).

In the first trial, the solution behaviour of compounds **1**–**3** was investigated. Compounds **1**–**3** exhibit very good solubility in organic solvents, such as acetonitrile. Compound **2** shows a typical monomer-like absorption spectrum with an intense π–π^* transition at $\lambda = 347$ nm, and a weak n–π^* transition near $\lambda = 440$ nm. Upon UV irradiation at $\lambda = 365$ nm for 1 h, a clear decrease at $\lambda = 347$ nm and, at the same time, an increase in the absorbance at $\lambda = 438$ nm can be observed; this is due to the conformational switching of the azo moieties from a *trans* to *cis* geometry. The absorbance decrease at $\lambda = 347$ nm could be fitted to a first-order equation with $R^2 = 0.9972$ and the reversibility of the *trans–cis* isomerisation of the azo groups in **2** could be followed through successive irradiations at $\lambda =$ 365 nm and with visible light. In the case of **1** and **3**, the *trans* state is transformed into the *cis* state upon irradiation, which can be explained in a similar way to that of **2** (Figures S4 and S5 in the Supporting Information). UV/Vis spectroscopic studies confirm the photo-isomerisation change of the as-prepared compounds **1**–**3**.

Because compounds **1**–**3** contain a hydrophilic POM head group, the hydrophobic alkyl chains and azobenzene moieties, an investigation into the aggregation behaviour of these amphiphilic compounds was performed in mixed co-solvents of CH_3CN/H_2O. For example, the slow addition of deionised H_2O into a solution of **2** in CH_3CN leads to the formation of a number of transparent orange solutions with different CH_3CN/H_2O (v/v) ratios of 8:2, 7:3, 5:5, 3:7 and 2:8. SEM measurements of **2** prepared from a $CH_3CN/H_2O = 7:3$ solution shows nanospherical morphology with diameters in the range of 300–400 nm (Figure 2a). With the change in the CH_3CN/H_2O ratio to 5:5 and 3:7, the SEM images exhibit similar nanospheres in these co-solvents (Figure 2b,c); TEM images also confirm the nanospherical morphology of **2** with a diameter of (350 ± 50) nm (Figure 2d,e) as well as DLS studies from $CH_3CN/H_2O = 5:5$ indicating an average diameter of 360 nm.

Detailed examination of the SEM images reveals that 1) the nanospherical particles are in close contact; and 2) a tiny hole can be observed on each of these nanospheres, suggesting that these nanospheres have a nonporous interior. It should be noted that for compound **2**, similar nanospherical particles can be obtained in different CH_3CN/H_2O co-solvent ratios, and the particles survive the relatively harsh vacuum environment required for the SEM and TEM measurements.

In $CH_3CN/H_2O = 7:3$, SEM images of compound **3** show nanospherical morphology with sizes of about 250 nm (Figure 3a). TEM images exhibit spherical particles in the range of 200 to 280 nm. The surface of these nanoparticles is very smooth and the adjacent nanoparticles are in close contact (Figure 3b,c). By adjusting the CH_3CN/H_2O ratio to 3:7, SEM images of compound **3** show that uniformly segmented nanorods can be observed (Figure 3d,e). TEM images of **3** provide further support for the self-organisation into nanorods of several micrometres long and tens of nanometres wide. The 1D nanostructures could overlap and entangle with each other. Furthermore, these rods appear to be relatively uniform, as evidenced by AFM (see the Supporting Information). When the ratio of CH_3CN/H_2O is 5:5, SEM images of **3** show that the surface of the particles exhibit clear curvature (Figure 3g). It can be seen clearly that 0D to 1D switching of compound **3** could be achieved at the nanoscale in mixed CH_3CN/H_2O solvents.

As shown in Figure 4, high-resolution transmission electron microscopy (HRTEM) images of **3** show a number of spherical nanoparticles with diameters of 2–3 nm. It should be noted that the crystalline texture could be observed (Figure 4b). Moreover, these spheres are closely dispersed. With an increase in the water content, the HRTEM images (Figure 4c,d) indicate

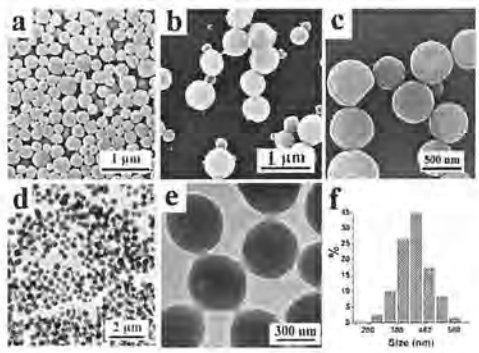

Figure 2. SEM images of **2** in 7:3 (a), 5:5 (b) and 3:7 (c) CH_3CN/H_2O. TEM images in 7:3 (d) and 3:7 (e) CH_3CN/H_2O. f) dynamic light scattering (DLS) results for **2** in $CH_3CN/H_2O = 5:5$.

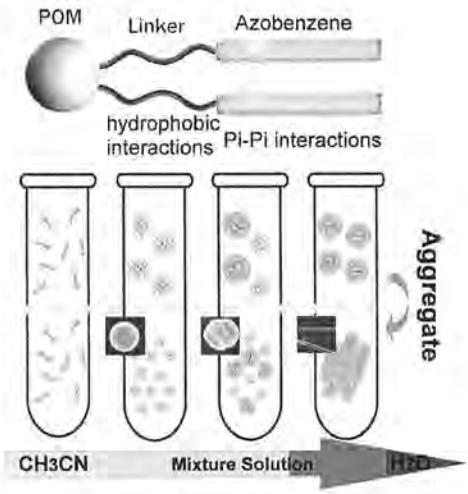

Figure 5. The designed POM assemblies with involvement of hydrophobic and π–π interactions, and the morphology and dimension control in CH_3CN/H_2O co-solvents.

tectures in co-solvent mixtures defines the basis of understanding the mechanism of the assembly, which allows us to design POM-based nanostructures for specific interactions.

Experimental Section

Compound **2** was synthesised by reaction of $[C_{16}H_{36}N]_4[SiW_{11}O_{40}(SiCH_2CH_2CH_2NH_2{\cdot}HCl)_2]$ (1.0 equiv), Et_3N (4.0 equiv) and 6-[4-(phenyldiazenyl)phenoxy]hexanoyl chloride (2.2 equiv) in acetonitrile below 5 °C. The solution was stirred at room temperature for 12 h, and then at 50 °C for 1 h. Deionised water (50 mL) was added to stop the reaction. The solvents were removed in vacuo to give a solid precipitate was obtained. The solid was filtered; washed with deionised water, ethanol and diethyl ether several times; and dried in air. The crude product was purified by recrystallisation from acetonitrile. Yield: 85%; ^{1}H NMR ($[D_3]CD_3CN$, 400 MHz): δ = 7.88 (d, 4H; ArH), 7.84 (d, 4H; ArH), 7.53 (t, 4H; ArH), 7.47 (t, 2H; ArH), 7.07 (d, 4H; ArH), 4.08 (t, 4H; CH_2), 3.22 (t, 4H; CH_2), 3.11 (t, 32H; CH_2), 2.15 (t, 4H; CH_2), 1.79 (s, 4H; CH_2), 1.72 (s, 8H; CH_2), 1.46 (s, 4H; CH_3), 1.61 (s, 32H; CH_2), 1.36 (m, 32H; CH_2), 0.96 (t, 48H; CH_3), 0.67 ppm (t, 4H; CH_2); ^{13}C NMR ($[D_3]CD_3CN$, 100 MHz): δ = 173.9, 162.8, 153.5, 147.4, 131.4, 130.1, 125.5, 123.1, 115.9, 69.2, 59.2, 42.1, 36.3, 29.5, 26.2, 24.3, 23.7, 20.2, 13.8, 10.8 ppm; IR (KBr): $\tilde{\nu}$ = 3404 (w), 2961 (m), 2873 (m), 1660 (m), 1599 (m), 1483 (m), 1380 (m), 1105 (m), 1043 (s), 964 (s), 947 (s), 903 (vs), 854 (m), 804 (s), 533 (m), 420 cm^{-1}; ESI-MS (CH_3CN, negative mode): *m/z*: 1968 $[2-2TBA]^{2-}$, 1846 $[2-3TBA+H)]^{2-}$; elemental analysis calcd (%) for $C_{106}H_{195}N_{10}O_{44}Si_3W_{11}$ (4420.73): C 28.80, H 4.47, N 3.17; found: C 28.29, H 4.14, N 2.93 (w). Detailed synthetic information for compounds **1** and **3** can be found in the Supporting Information.

Acknowledgements

This research was supported by the National Science Foundation of China (21222104, 21076020), the Beijing Nova Program (2009B12), and the Fundamental Research Funds for the Central Universities (ZZ1227).

Keywords: azo compounds · noncovalent interactions · polyoxometalates · self-assembly · supramolecular chemistry

[1] a) H. N. Miras, J. Yan, D. L. Long, L. Cronin, *Chem. Soc. Rev.* **2012**, *41*, 7403–7430; b) D.-L. Long, R. Tsunashima, L. Cronin, *Angew. Chem.* **2010**, *122*, 1780–1803; *Angew. Chem. Int. Ed.* **2010**, *49*, 1736–1758; c) Y.-F. Song, R. Tsunashima, *Chem. Soc. Rev.* **2012**, *41*, 7384–7402; d) A. Proust, R. Thouvenot, P. Gouzerh, *Chem. Commun.* **2008**, 1837–1852; e) A. Proust, B. Matt, R. Villanneau, G. Guillemot, P. Gouzerh, G. Izzet, *Chem. Soc. Rev.* **2012**, *41*, 7605–7622; f) A. Dolbecq, E. Dumas, C. R. Mayer, P. Mialane, *Chem. Rev.* **2010**, *110*, 6009–6048.

[2] a) Y.-F. Song, D.-L. Long, L. Cronin, *Angew. Chem.* **2007**, *119*, 3974–3978; *Angew. Chem. Int. Ed.* **2007**, *46*, 3900–3904; b) C. P. Pradeep, D.-L. Long, C. Streb, L. Cronin, *J. Am. Chem. Soc.* **2008**, *130*, 14946–14947; c) Y.-F. Song, D.-L. Long, C. Ritchie, L. Cronin, *Chem. Rec.* **2011**, *11*, 158–171; d) Y.-F. Song, D.-L. Long, L. Cronin, *CrystEngComm* **2010**, *12*, 109–115.

[3] a) S.-T. Zheng, J. Zhang, X.-X. Li, W.-H. Fang, G.-Y. Yang, *J. Am. Chem. Soc.* **2010**, *132*, 15102–15103; b) S.-T. Zheng, J. Zhang, G.-Y. Yang, *Angew. Chem.* **2008**, *120*, 3973–3977; *Angew. Chem. Int. Ed.* **2008**, *47*, 3909–3913; c) J.-W. Zhao, C.-M. Wang, J. Zhang, S.-T. Zheng, G.-Y. Yang, *Chem. Eur. J.* **2008**, *14*, 9223–9239; d) S.-T. Zheng, J. Zhang, J. M. Clemente-Juan, D.-Q. Yuan, G.-Y. Yang, *Angew. Chem.* **2009**, *121*, 7312–7315; *Angew. Chem. Int. Ed.* **2009**, *48*, 7176–7179; e) J. Zhou, J. Zhang, W.-H. Fang, G.-Y. Yang, *Chem. Eur. J.* **2010**, *16*, 13253–13261.

[4] a) T. Liu, M. L. K. Langston, D. Li, J. M. Pigga, C. Pichon, A. M. Todea, A. Müller, *Science* **2011**, *331*, 1590–1592; b) J. Zhang, Y.-F. Song, L. Cronin, T. B. Liu, *J. Am. Chem. Soc.* **2008**, *130*, 14408–14409; c) J. Zhang, Y.-F. Song, L. Cronin, T. B. Liu, *Chem. Eur. J.* **2010**, *16*, 11320–11324; d) C. P. Pradeep, M. F. Misdrahi, F.-Y. Li, J. Zhang, L. Xu, D.-L. Long, T. Liu, L. Cronin, *Angew. Chem.* **2009**, *121*, 8459–8463; *Angew. Chem. Int. Ed.* **2009**, *48*, 8309–8313; e) P. Yin, D. Li, T. Liu, *Chem. Soc. Rev.* **2012**, *41*, 7368–7383.

[5] a) G. M. Whitesides, J. P. Mathias, C. T. Seto, *Science* **1991**, *254*, 1312–1319; b) J.-M. Lehn, *Supramolecular Chemistry: Concepts and Perspectives*, Wiley-VCH, Weinheim, **1995**.

[6] a) S. Landsmann, C. Lizandara-Pueyo, S. Polarz, *J. Am. Chem. Soc.* **2010**, *132*, 5315–5321; b) S. Landsmann, M. Wessig, M. Schmid, H. Colfen, S. Polarz, *Angew. Chem.* **2012**, *124*, 6097–6101; *Angew. Chem. Int. Ed.* **2012**, *51*, 5995–5999.

[7] a) Y.-F. Song, N. McMillan, D.-L. Long, S. Kane, J. Malm, M. O. Riehle, C. P. Pradeep, N. Gadegaard, L. Cronin, *J. Am. Chem. Soc.* **2009**, *131*, 1340–1341; b) Y.-F. Song, N. McMillan, D.-L. Long, T. Thiel, Y. L. Ding, H. S. Chen, N. Gadegaard, L. Cronin, *Chem. Eur. J.* **2008**, *14*, 2349–2354.

[8] J. Thiel, D.-M. Yang, M. H. Rosnes, X. Liu, C. Yvon, S. E. Kelly, Y.-F. Song, D.-L. Long, L. Cronin, *Angew. Chem.* **2011**, *123*, 9033–9037; *Angew. Chem. Int. Ed.* **2011**, *50*, 8871–8875.

[9] Y.-F. Song, D.-L. Long, S. E. Kelly, L. Cronin, *Inorg. Chem.* **2008**, *47*, 9137–9139.

[10] G. M. Whitesides, M. Boncheva, *Proc. Natl. Acad. Sci. USA* **2002**, *99*, 4769–4774.

[11] J.-C. Eloi, D. A. Rider, G. Cambridge, G. R. Whittell, M. A. Winnik, I. Manners, *J. Am. Chem. Soc.* **2011**, *133*, 8903–8906.

[12] Y. Yan, H. B. Wang, B. Li, G. F. Hou, Z. D. Yin, L. X. Wu, V. W. W. Yam, *Angew. Chem.* **2010**, *122*, 9419–9422; *Angew. Chem. Int. Ed.* **2010**, *49*, 9233–9236.

[13] I. Bar-Nahum, H. Cohen, R. Neumann, *Inorg. Chem.* **2003**, *42*, 3677–3684.

[14] a) J. N. Israelachvili, D. J. Mitchell, B. W. Ninham, *J. Chem. Soc. Faraday Trans. 2* **1976**, *72*, 1525–1568; b) R. Nagarajan, *Langmuir* **2002**, *18*, 31–38.

[15] D. Chandler, *Nature* **2005**, *437*, 640–647.

[16] D. Myers, *Surfaces, Interfaces, and Colliods: Principles and Applications, 2nd ed.*, Wiley-VCH, Weinheim, **1999**.

Received: July 8, 2013
Published online on August 5, 2013